Laboratory Course on Silicon Sensors

Elisabetta Crescio and Marek Idzik

INFN, Torino, Italy

Danielle Moraes and Alan Rudge

CERN, CH-1211, Geneva, Switzerland

This laboratory course consists of five different mini sessions, in order to give the student some hands-on experience on various aspects of silicon sensors and related integrated electronics. The five experiments are:

- Characterization of silicon detectors (VCI measurements).
- Double light spot (measurement of the collection time of electron and holes separately versus voltage in a silicon diode).
- Understanding of the operation of the VA read-out chip, and measurement of its noise versus detector capacitance characteristics.
- Measurement of the position resolution of a microstrip detector.
- Observation of spectra in a silicon diode.

I. CHARACTERIZATION OF SILICON DIODES FOR PARTICLE DETECTION

A. Introduction

Near intrinsic n-type silicon with a metallised p-doped region is the most frequently used semiconductor structure for detecting charged tracks in high-energy physics exepriments. A polarisation voltage is applied across the diode structure, which depletes the silicon from charge carriers. Charged particles or photons interacting with the silicon will create electron-hole pairs that drift along the electric field lines to the contacts located on the silicon surface. A schematic picture of a silicon sensor diode is shown in fig.1.

A first step in constructing a particle detector based upon a silicon sensor is to characterise the sensor without readout electronics attached. The static characteristics of a sensor are usually adequate to determine if the sensor can be used for particle detection. The leakage current behaviour as a function of voltage and the voltage needed to fully deplete the sensor are two important parameters. The voltage needed to fully deplete the sensor can be determined by measuring the capacitance between the diode implant and the back-plane of the sensor. In the final particle detector system, both the capacitance and the leakage current will influence the performance of the readout electronics. The capacitance and leakage current depend on the geometry of the sensor and the quality of the material and manufactoring process. In a well controlled and uniform process sensors with the same geometrical layout, processed on the same substrate, should have the same behaviour. In reality, there may be variation both in the process and in material and therefore there may be sensors which differ largely from what we naively would expect. When constructing and

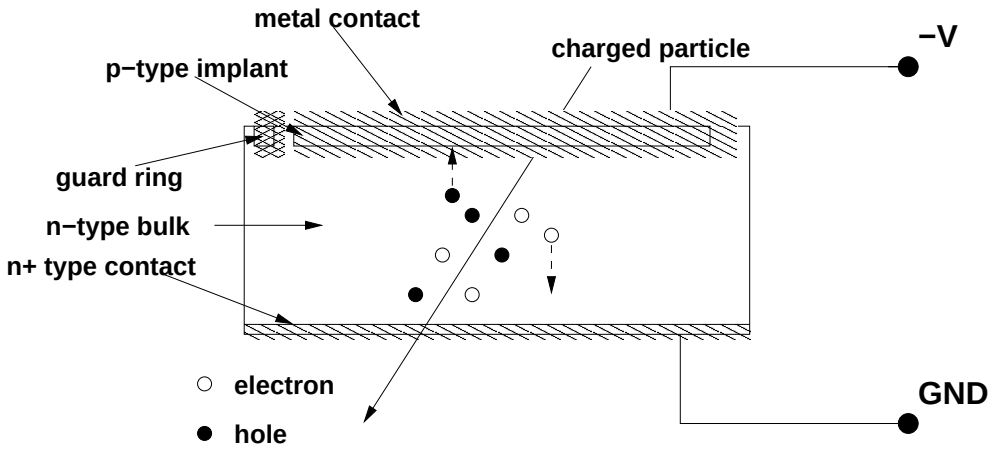

FIG. 1: A schematic picture of a silicon sensor diode.

experiment consisting of many sensors we have to measure them in the laboratory to find the good sensors that can be built into the experiment.

This session requires some knowledge of the basic principles of diodes and will give experience handling unprotected diodes, operating the microscope and probe manipulators. Because of the short time available we restrict ourselves to simple DC-coupled diodes.

B. Laboratory setup

In this experiment we use the following equipment:

- probe station;
- digital multimeter;
- capacitance meter and power supply;
- vacuum pump;
- microscope;

In fig.2 a schematic picture of the setup is shown.

C. Measurement of IV-properties of silicon diodes at room temperature

The main sources of leakage current in silicon sensors are:

1. Diffusion of charge carriers from undepleted regions of the detector to the depleted region.
2. Thermal generation of electron-hole pairs in the depleted region.
3. Surface currents depending on contamination, surface defects from processing and edge effect from dicing, etc.

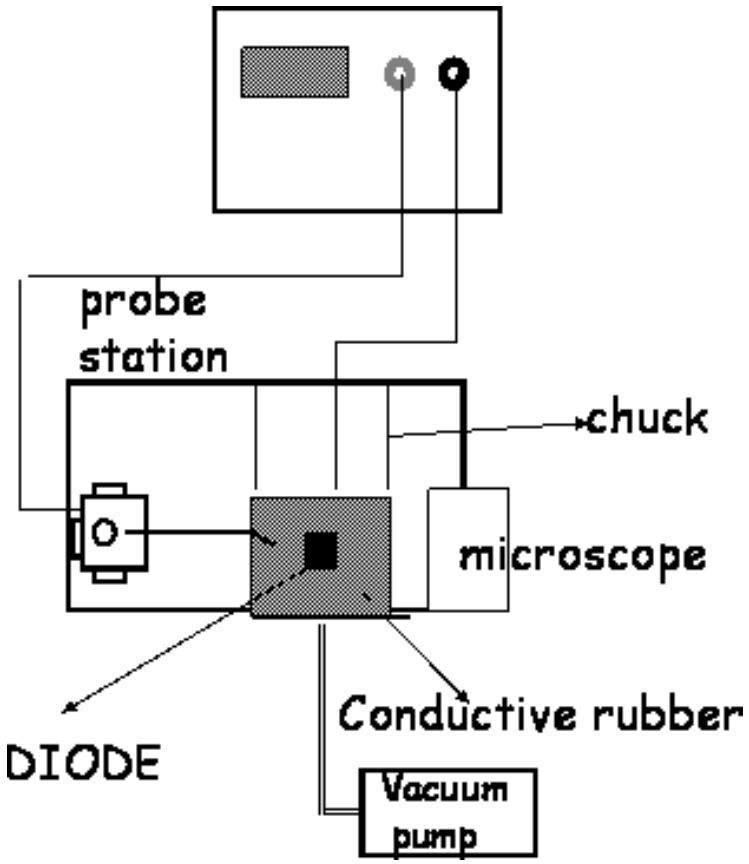

FIG. 2: A schematic picture of the setup of CV and IV measurement.

Contribution (1) is generally well controlled and small giving a few nA/cm^2. The contribution from (2) depends largely on the purity of the material since recombination centres and trapping centres increase the creation of electron-hole pairs. The magnitude is higher that for (1), giving a few μA/cm^2. The leakage current originating from thermal generation is of course temperature dependent. By lowering the temperature of the sensor we may reduce the contribution. By decreasing the temperature by 10^{o}C the leakage current will typically be reduced to a third. In some cases the contribution from (3) may be the dominant source of leakage current. The surface current may be caused by effects on the non-depleted edge region or by a bad processing environment. The leakage current originating from the surface may vary extensively from sensor to sensor. To reduce the effects from surface current a guard ring structure is processed on the silicon. The guard ring can be anything from a single implant around the diode to a complex structure of alternating implants and floating metal rings around the silicon diode. We will now study the IV-characteristic of a silicon diode sensor with 300 $\mu\, m$ thickness. Execute the steps below:

1. Place the silicon diode on the vacuum chuck with conductive rubber under it.
2. Connect the diode with the probe needle to the negative pole of the battery pack.
3. Connect the chuck (and thus, the silicon backplane) to the positive pole of the battery.
4. Cover the probe station to prevent light from generating current in the diodes, note down the voltage and current at 0 V.

5. Ramp up the voltage and note down the voltage and the corresponding current.

D. Measurement of CV-properties of silicon diodes at room temperature

At low reverse bias voltage the capacitance will fall such that $1/C^2$ is proportional to V. When the sensor has reached full depletion the capacitance will not change anymore. This is clearly visible when plotting $1/C^2$ vs. V. The point where the curve shows a kink and does not reduce further gives the point for full depletion. For large single diodes the capacitance to the backplane is the dominant contribution to the total capacitance. For small and segmented sensors such as pixel and microstrip sensors the inter pixel/strip capacitance will dominate over the backplane capacitance when the sensor is fully depleted. The inter pixel/strip capacitance do not change in the same way as the backplane capacitance when applying reverse bias to the sensor. In this experiment, the capacitance of the silicon diode is measured between the backplane and the p-implant. Execute the steps below:

1. Find the capacitance C_0 of the setup by leaving the circuit open.

2. Follow the procedure outlined for IV-measurements. Measure the full capacitance (capacitance of the diode and capacitance of the setup), calculate the capacitance of the diode by subtracting the value C_0 from the measured one, and note down the measurements.

E. Results from the measurments

The results obtained from the measurements are shown in table I E. The corresponding curves are shown in fig. 3. The silicon diode shows a strong increase in leakage current after 40V. This may indicate a breakdown in the structure. The capacitance decreases with higher depletion voltage, and the silicon diode shows the expected behaviour of capacitance vs. depletion voltage. At 60V the silicon diode shows full depletion.

TABLE I: IV and CV measurements.

Voltage[V]	Current[pA]	Capacitance[pF]	C_0
0	-12	51	38 pF
10	27	28	
20	56	18	
30	6	16	
40	86	13	
50	114	11	
60	132	10	
70	215	10	
80	360		

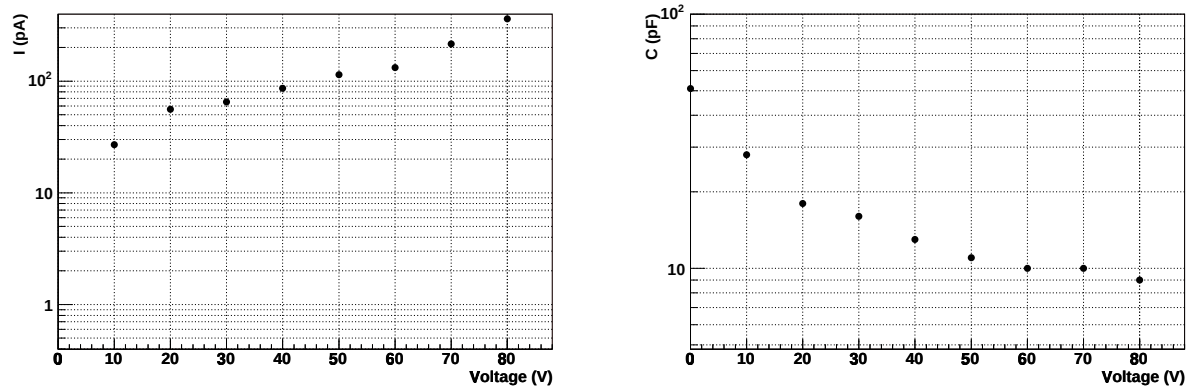

FIG. 3: The current of the diode as a function of the applied voltage (left) and the logarithm of the corrected capacitance vs. depletion voltage in V (right).

II. STUDY OF THE VIKING ARCHITECTURE AND NOISE PERFORMANCE

A. The Viking architecture

A number of readout methodologies exist. Among these, the principal ones are the MX series which use double correlated sampling, successfully used in the DELPHI vertex detector, and the Viking "time continuous" shaping. These are illustrated in fig. 4. The Amplex/Viking "time continuous" shaping is shown in fig. 5.

A voltage corresponding to the input charge is stored on the sample and hold capacitor and read out sequentially via the output multiplexer. It is important to understand the shift in/out concept to daisy chain many (up to 20) chips. Fig. 6 shows a timing diagram for the readout sequence of a Viking chip. Corresponding screen shots from a digital oscilloscope are shown in fig. 7(a) and fig. 7(b). Corresponding screen shots from a digital oscilloscope are shown in fig. 8(a) and 8(b).

An important mode of operation is the single channel mode, where the output is seen from one amplifier. This is shown in fig. 8(b) for a signal from an Americium source.

B. Study of noise performance of the Viking readout circuit

An essential part in operating silicon sensors is a low noise amplifier circuit. The energy needed to create an electron-hole pair at room temperature in silicon is around 3.6 eV. A minimum ionising particle traversing 300 μm of silicon will on average create 25000 electron-hole pairs. For low energy X-ray applications the requirements for low noise is even more demanding. A 10 KeV X-ray will only produce 2800 electron-hole pairs ini silicon. The main contribution of the silicon sensor to the total noise of the assembly comes from:

- the load capacitance of the silicon sensor;
- the leakage current in the silicon sensor;
- possible resistance between the active element of the sensor and ground, or the bias supply.

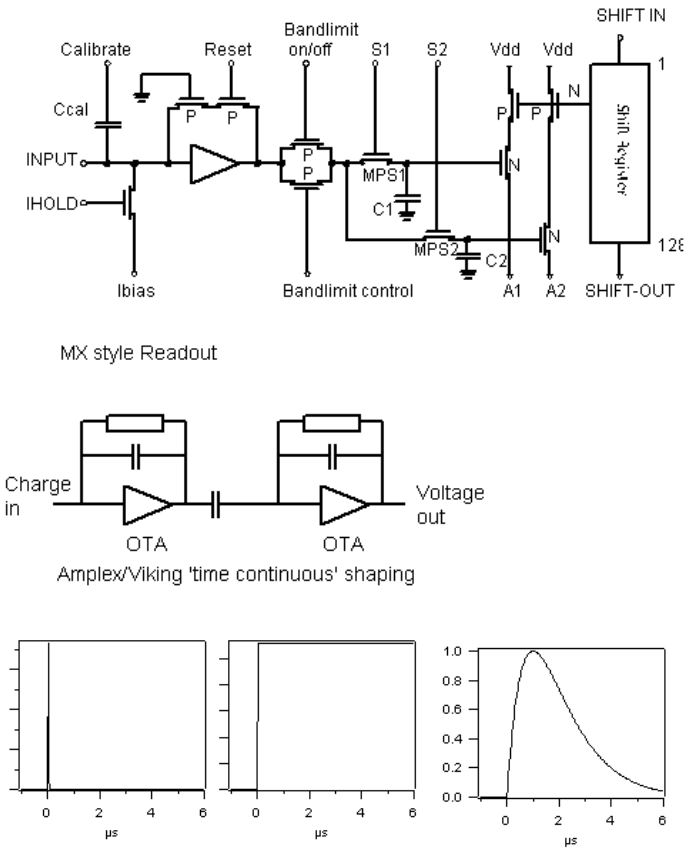

FIG. 4: The MX and Viking principle.

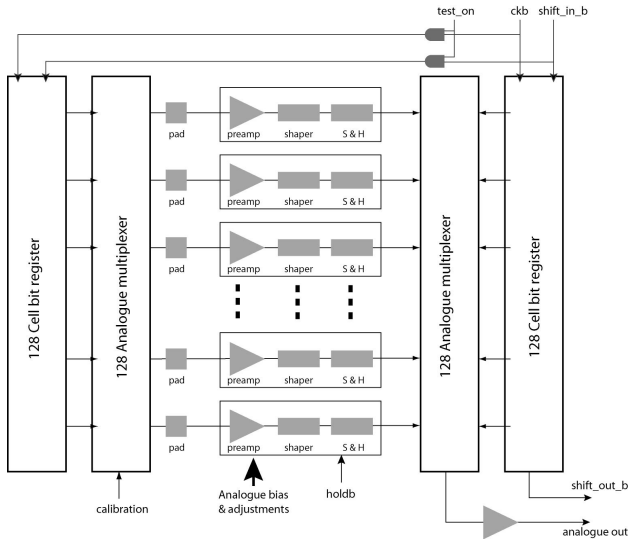

FIG. 5: The Amplex/Viking architecture.

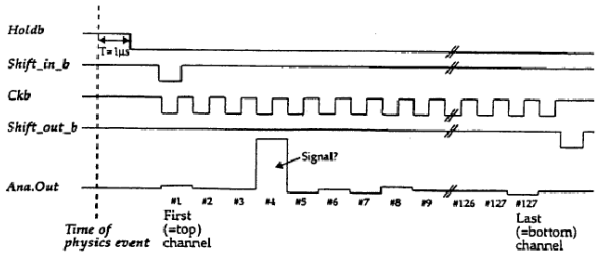

FIG. 6: Timing diagram for the readout sequence of a Viking chip.

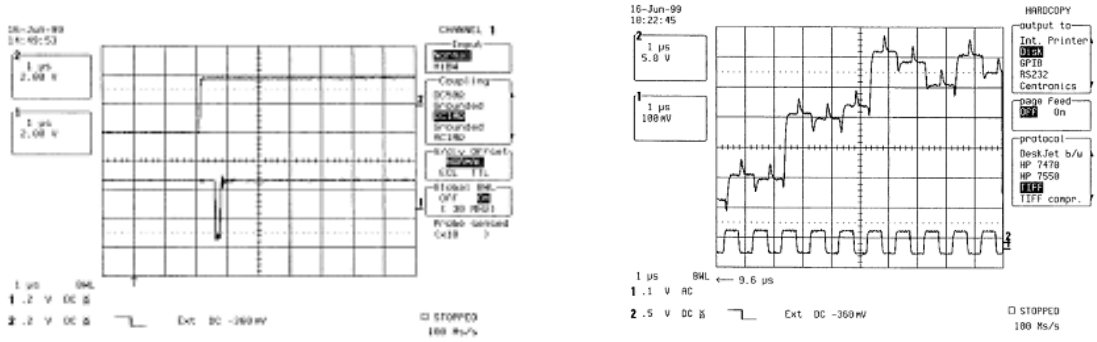

(a) (b)

FIG. 7: (a)Screen shots showing hold and shift signals. (b)Screen shots showing clocking and analogue output pulse.

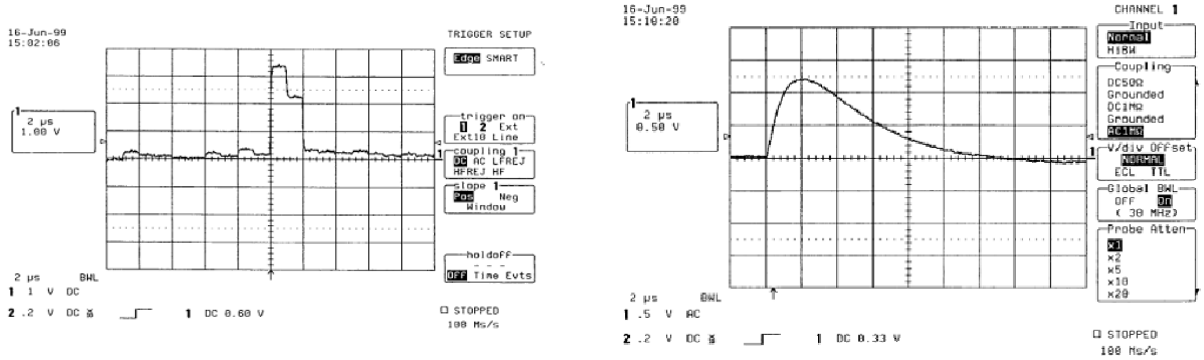

(a) (b)

FIG. 8: (a)Screen shots showing output waveform showing hits in two adjacent channels. (b)Output from a single channel.

The main sources of noise for silicon detector assemblies are: The Equivalent Noise Charge (ENC) of the input FET of the pre-amplifiers proportional to the load capacitance:

$$ENC_{FET} = \frac{Ce}{q}\sqrt{\frac{4kT}{3g_m\tau}} \tag{1}$$

The detector (and input FET) leakage noise:

$$ENC_l = \frac{e}{q}\sqrt{\frac{qI_l\tau}{4}} \tag{2}$$

The bias and feedback resistor noise:

$$ENC_R = \frac{e}{q}\sqrt{\frac{\tau kT}{2R}} \tag{3}$$

where C is the total load capacitance, I_l is the leakage current, τ is the peaking time of the amplifier, k the Boltzmann constant, T the absolute temperature in Kelvin and R is parallel of the bias resistor and feedback resistor. The total noise contribution is the squared sum of the components listed above:

$$ENC_{total} = \sqrt{ENC_{FET}^2 + ENC_l^2 + ENC_R^2} \tag{4}$$

For the Viking chip the noise is typically $70\,e^- + 12\,e^- C_{load}[pF]$. It is obvious that we want to keep the leakage current small by choosing a sensor that has low leakage current at a voltage that fully depletes the sensor. The contribution to the noise from the detector capacitance and series resistance will be studied in this experiment.

C. Laboratory setup

In this session we use the following equipment:

1. Timing unit for readout circuit, VIKING TIMING;
2. Pulse generator for trigger;
3. Current limited power supply for readout circuit;
4. NIM crate;
5. Digital oscilloscope capable of measuring RMS.

We have an assembly with a Viking chip connected to capacitors of various values.

D. Measurement

In order to measure the noise, the setup has to be calibrated. This is done by applying a known charge pulse Q_{cal} on the input of the Viking chip and measuring the output from

the chip V_{outl}. The input charge is generated by applying a known voltage pulse V_{cal} over a known calibration capacitor C_{cal}:

$$Q_{cal} = \frac{C_{cal} V cal}{e} \tag{5}$$

where e is here the magnitude of the electron charge ($e = 1.6 \times 10^{-19} C$. The calibration capacitance C_{cal} is on our case 1.8 pF. The RMS of the noise V_{noise} from the Viking chip without test pulse in mV can be calculated using a modern digital oscilloscope. Since the calibration is known, the measured value in mV can be converted to ENC by the relation:

$$ENC = \frac{V_{noise} Q_{cal}}{V_{out}} \quad RMS\, e \tag{6}$$

Six channels have been pre-wired with different load capacitances to the input pads of the Viking chip. Determine the calibration and measure the corresponding ENC noise for the channels, and note down the values.

E. Results from the measurement

The measured values are reported in table IIE. The plot of noise vs. capacitance is

TABLE II: Values of the measured noise.

Capacitance[pF]	V_{cal}[mV]	V_{out}[mV]	V_{noise}[RMS mV]	ENC[RMS e^-]
0	2	2500	10	90
3	2	2500	13	115
13	2	2500	28	250
25	2	2300	43	420
36	2	2200	60	600
51	2	2000	78	880

shown in fig. 9.

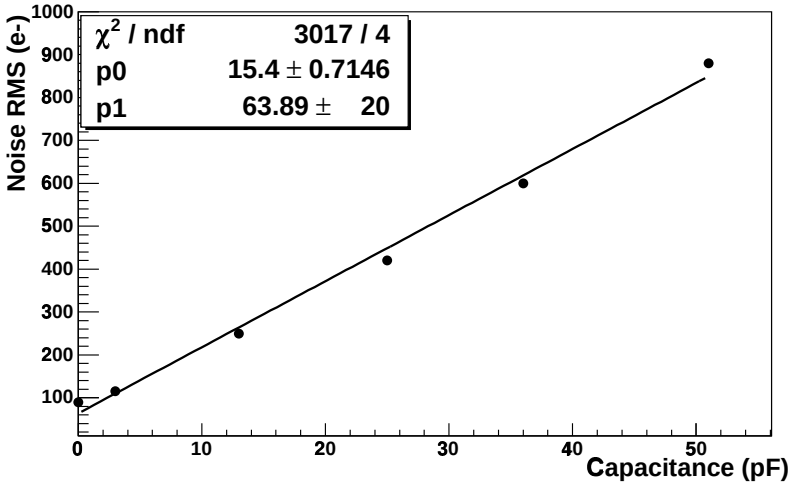

FIG. 9: VA2 noise vs. detector capacitance.

III. STUDY OF THE POSITION RESOLUTION OF A SILICON MICROSTRIP DETECTOR

A. Introduction

Silicon microstrip sensors are the most commonly used device for high resolution tracking in particle physics. The strip design allows a large sensitive area with relatively few readout channels. The basic strip detector is read out on one side giving information of the track position only in one dimension. Various solutions to measure track position in two dimensions exist. The simplest solution is to glue two single-sided sensors back-to-back, but a more demanding design is to process strips on both sides of the sensor. In this experiment we will study a single sided sensor which is illuminated by a pulsed laser source on the strip side (because the back of the sensor is fully aluminised).

B. The laboratory setup

In this experiment we use the following equipment:

1. Timing unit for readout circuit, VIKING TIMING;
2. Pulse generator for trigger and laser;
3. Current limited power supply for readout circuit;
4. NIM crate;
5. Oscilloscope;
6. Laser diode driver;
7. Battery pack for biasing the sensor;

The silicon microstrip sensor is wire bonded to the Viking readout circuit, which has been placed on a readout PCB (Printed Circuit Board). The assembly has been mounted on a slide which can be precisely moved such that the translation direction is orthogonal to the strips. An optical fibre has been mounted about 100 μm away from the silicon surface. Fig. 10 shows a photograph of the PCB card and the detector mounted on the slide.

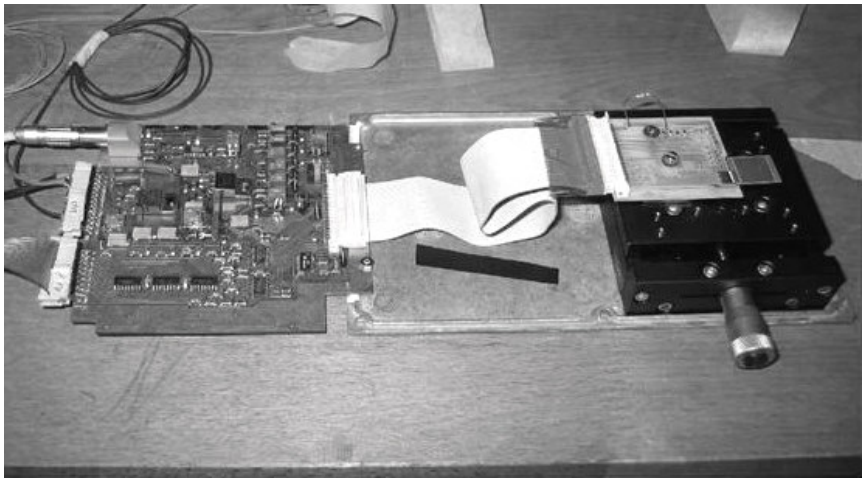

FIG. 10: Picture of the PCB board and the detector mounted on the slide.

C. Measurement

We will now try to determine the position resolution of the silicon microstrip sensor. The peak of the light source is a few several strips wide. We require the information from a number of strips in order to accurately determine the peak position. By moving the fibre closer to the silicon sensor the laser spot size will reduce, but on the other hand we risk mechanically damaging the sensor.Proceed as floows:

1. move the slide by turning the micrometer screw on the right hand side of the box (seen from the repeater electronics board). You will now see the signal from the light move from one strip to another. You may also notice that this translation is not very smooth. The reason for this is the aluminium on top of the implanted strips which reflect a fraction of the light and reduces the signal locally. This effect would be larger if we had a better focused light spot.

2. Place the sensor in a region with a nicely distributed signal.

3. Determine and write down the amplitudes of the channels in the peak by moving the cursor on the oscilloscope.

4. Four complete turns of the screw correspond to 1 mm. Therefore one major division equals 10 μm. Move the slide by 10 μm and repeat 3.

5. Repeat 4. and 3.

D. Results from the measurement

Table III D shows the measured amplitudes of the signal for different positions of the sensor. Fig. 11 shows the oscilloscope output without a laser spot (a), and with the laser

TABLE III: Raw data from the setup.

Strip n	0 μm	10 μm	20 μm	30 μm	40 μm	50 μm
1	304	292	268	240	232	212
2	424	400	368	340	320	288
3	612	584	544	504	472	436
4	888	844	808	760	716	680
5	1030	1000	984	948	912	884
6	1150	1140	1130	1100	1080	1050
7	1140	1160	1170	1150	1130	1120
8	1010	1070	1100	1130	1160	1200
9	736	772	820	864	916	968

spot in two different positions (b and c).

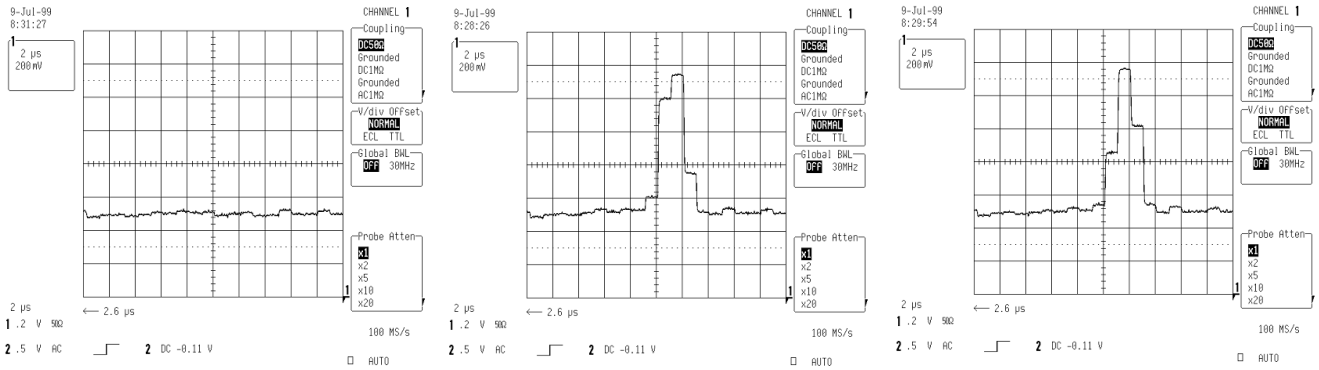

(a) (b) (c)

FIG. 11: Oscilloscope output without a laser spot (a), and with the laser spot in two different positions (b and c).

One horizontal division corresponds to about two readout channels. Now perform a gaussian fit for each position and calculate the peak positions. Table III D shows the results from a previous measurement. ositions of the sensor. Since we are averaging the signals from

TABLE IV: Results from the position resolution measurement (in μm).

	0 μm	10 μm	20 μm	30 μm	40 μm	50 μm
Calculated peak	264	274	282	292	302	312
Difference		10	8	10	10	10

the Viking in order to minimize the electronics noise, and taking 10 points to determine the peak in the gaussian fit, it can be seen that position accuracy down to a few μm can be achieved. What are the main error sources?

IV. STUDY OF CHARGE TRANSPORT IN SILICON WITH A FAST AMPLIFIER

A. Introduction

In gaseous detectors the mobility for electrons is several orders of magnitude higher than for positive ions. In semiconductors the mobility for holes is only slightly lower than for electrons. In general the signal propagation in semiconductors is a few nanoseconds while the signal propagation in gaseous detectors typically varies from microseconds to milliseconds. In order to study the drifting of electron and holes in silicon, very fast electronics is required. The drift velocity for electrons and holes in silicon at low electric field strength is given by:

$$v_e = \mu_e E \tag{7}$$

$$v_h = \mu_h E \tag{8}$$

where μ_e and μ_h are the mobilities for electrons and holes respectively, and E is the electric field. The mobility in silicon at room temperature is 1350 cm^2/Vs for electrons, and 480 cm^2/Vs for holes. At high field the velocity saturates with velocities of the order of 10^7 cm/s. When the sensor is fully depleted, the signals from holes and electrons will arrive almost at the same time. We can try to study the slower transit of holes by shining a short laser pulse on the back side of a non-depleted n-type silicon diode. By choosing a wavelength which does not penetrate far in the silicon the charge can be generated close to the surface of the silicon. The holes have now to drift to the other side of the sensor, while the electrons are formed at the interface. If the electric field is low and the detector has a reasonably large depleted region we will now see a difference in the total time between the signal arising from electrons and holes. It is important to realise that the signal itself arises *immediately* the charge carriers start to move, and lasts until the last charge carriers are collected.
By starting with a high depletion voltage the signal from the setup will have the same shape as the light pulse from the laser which is shown in fig.12.

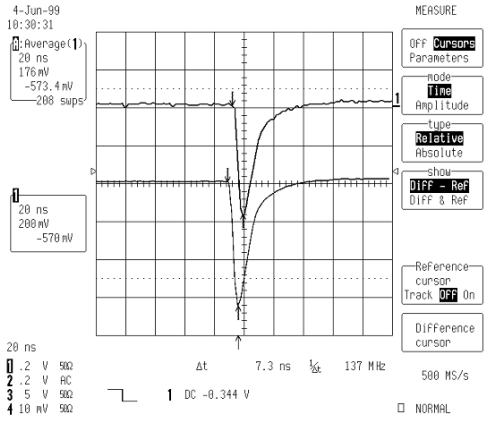

FIG. 12: The amplifier output from the laser pulse with a fully depleted silicon diode.

The current signal which is induced on the diode is due to the movement of both charge carriers in the electric field. The transit time for the carriers can be calculated by integrating

equations 7 and , remembering that the field varies as a function of position:

$$E(x) = \frac{qN_D}{\epsilon}x + E_{min} \tag{9}$$

where E_{min} is a function of the bias voltage, and is a minimum of zero for a barely depleted detector, then the transit times are:

$$t_h = \frac{\epsilon}{\mu_h N_D} ln\Big(\frac{w + (\epsilon/qN_D)E_{min}}{x_0 + (\epsilon/qN_D)E_{min}}\Big) \tag{10}$$

$$t_e = \frac{\epsilon}{\mu_h N_D} ln\Big(\frac{x_0 + (\epsilon/qN_D)E_{min}}{(\epsilon/qN_D)E_{min}}\Big) \tag{11}$$

where x_0 is the depth of production, measured from the ohmic contact side. The induced current is given by Ramos theorem, which states that the current on the electrode of interest is equal to the charge value multiplied by the dot product of the "weighting field" and the charge velocity. The weighting field is an hypothetical field calculated by putting unit potential on the electrode of interest, zero on all other electrodes, and ignoring any static charges (N_D in our case). For a simple diode, this reduces to a constant 1/w, and the velocities are aligned with the electric field, so calculating the scalar velocities gives the induced current:

$$i_h = q\frac{1}{w}\mu_h\Big(E_{min} + \frac{x_0 qN_D)}{\epsilon}\Big)\Big(exp\Big[\mu_h q\frac{N_D}{\epsilon}t\Big]\Big) \tag{12}$$

$$i_e = q\frac{1}{w}\mu_e\Big(E_{min} + \frac{x_0 qN_D)}{\epsilon}\Big)\Big(exp\Big[-\mu_e q\frac{N_D}{\epsilon}t\Big]\Big) \tag{13}$$

In fact these pulses become smeared by the amplifier bandwidth, and the resulting pulse is what is seen on the oscilloscope.

B. The setup

In this experiment we use a fast amplifier chain connected to a diode of n-type silicon with the backplane not covered by aluminium. Two light fibres lead the laser light to the two opposite sides of the diodes. A picture of the sensor setup, with a zoom of the sensor region, is shown in fig.13. Other equipment used are:

1. Oscilloscope;
2. Laser diode driver;
3. Battery pack for biasing the sensor;
4. Pulse generator for trigger and laser;
5. Low voltage power supply;
6. NIM crate.

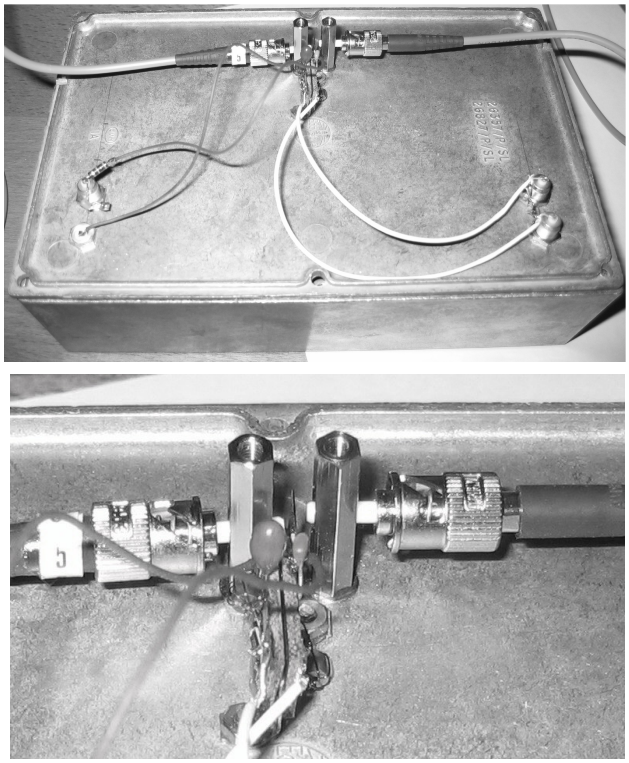

FIG. 13: Picture of the sensor setup.

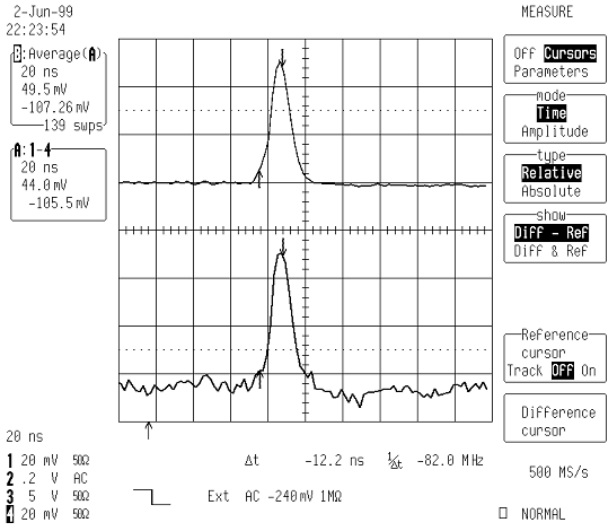

FIG. 14: The signal from a unbiased sensor (read out from the p-side) when laser shined on the p-side.

C. Signals when shining laser on the junction side (p-side)

With the laser pulse on the p-side, you get the picture on oscilloscope shown in fig. 14. Turn on the sensor bias and ramp slowly up the voltage. The amplitude of the signal gets larger but the shape stays approximately unchanged. The sensor is depleted from the p-side

and the n-side is conducting transporting the electrons to the amplifier.

D. Signals when shining laser on the backplane (n-side)

When the pulse is incident on the n-side and the detector is off, there is a very tiny signal. The holes are trapped close to the backplane. As the bias is increased, one sees an increasing signal (see fig. 15), with a double peak structure. In the double peak structure are visible the contribution coming from fast arriving electrons and the contribution from holes with a lower mobility which have to travel through the depleted region of the sensor. The double peak structure disappears when the bias voltage gets higher. At full depletion

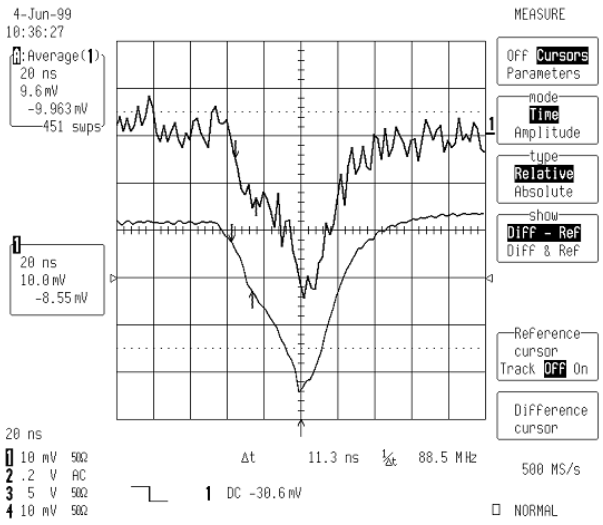

FIG. 15: The signal amplitude at low bias voltage when laser shined on n-side of the silicon sensor (The signal is read out from the n-side).

the amplitude of the signal is comparable when laser shined on p and n sides (see fig. 16).

The optical fibre cables are not labeled;can you decide by using one or the other cable, which cable points on the n-side, and which on the p-side?

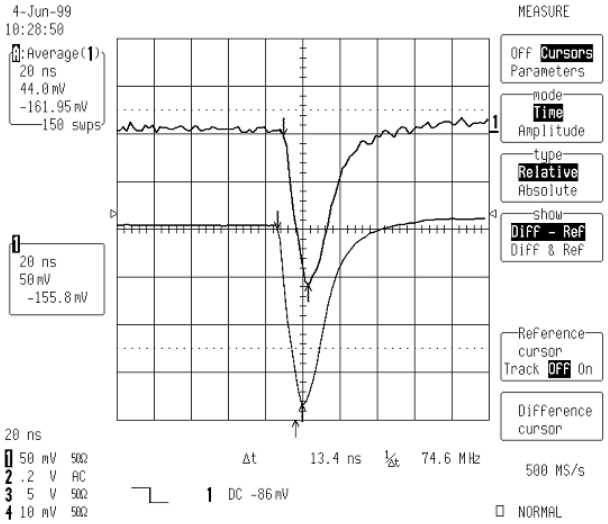

FIG. 16: The signal amplitude at full depletion when laser is shined on n-side (read out from n-side).

V. SPECTROSCOPY WITH THE VIKING CHIP AND PAD DETECTOR

A. Introduction

During this experiment we will use a silicon sensor to see the spectrum form a γ source and study its energy resolution.

B. The setup

The VIKING chip is used in single channel mode and the inputs bonded to a small silicon detector with 36 pads of 1 mm square. Channel 12 is bonded to 1 pad, channel 36 to 2 pads, channel 58 to 4 pads, channel 78 to 8 pads and channel 102 to 21 pads. The other equipment used in this experiment is the following:

1. Oscilloscope;
2. $^{2}41$Am source;
3. Battery pack for biasing the sensor;
4. Viking Timing unit;
5. Low voltage power supply;
6. NIM crate.
7. Multi Channel Analyzer and PC.

A picture of the sensor setup is shown in fig. 17.

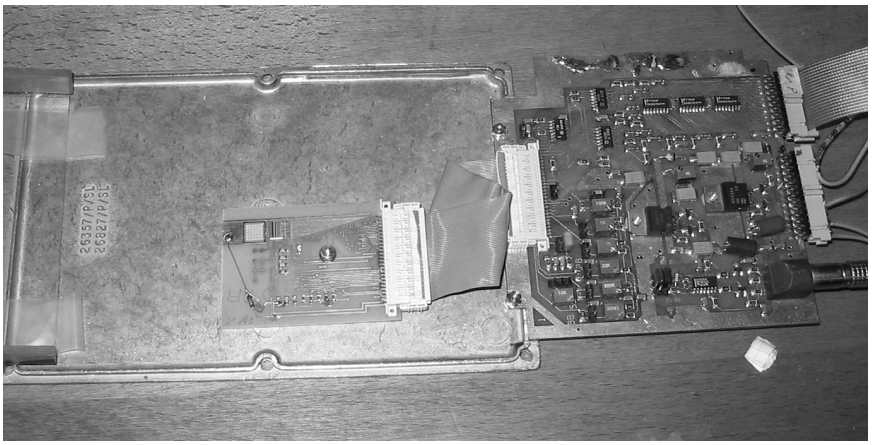

FIG. 17: Photograph of the setup. The sensor and the readout chip are mounted on a printed circuit board which is placed into a aluminium box.

C. The measurement

A spectrum of ^{2}41Am is taken with channel 12 (only one pad) with the Am source placed under the printed circuit board hosting the detector. The spectrum is shown in fig. 18. The peak corresponding to the 59.95 X-ray line is clearly visible at channel 54. Since the detector is supported on the board with copper and the contact to the backplane of the sensor is done with silver loaded glue, other peaks at lower energies are observed, corresponding to florescence lines excited by the 59.95 keV line from copper and silver. The K_α and K_β lines for copper and silver are: Cu (K_α) 8.03 keV, Cu (K_β) 8.90 keV, Ag (K_α) 21.99 keV and Ag (K_β) 24.94 keV.

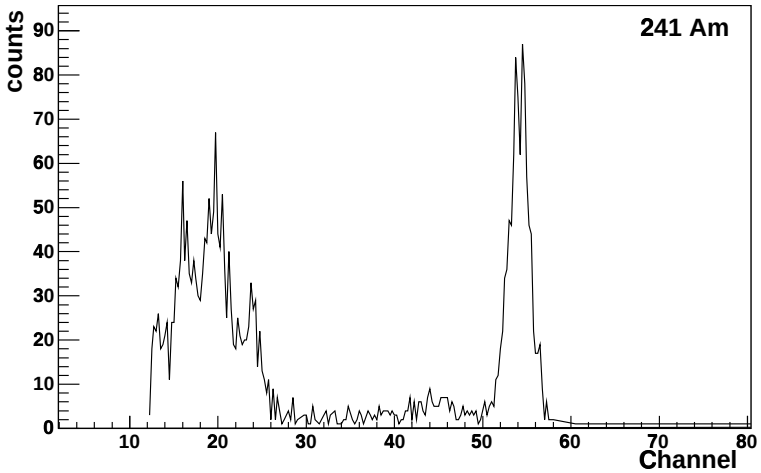

FIG. 18: Spectrum from a ^{2}41Am source. The source is placed under the printed circuit board hosting the detector.

Successively, other measurement are taken with the source placed into the aluminium box on a "bridge" above the sensor. In this case only the peak corresponding to the 59.95

keV line is visible. In the following, the peaks obtained reading out channels 12,36,58,78,102 are shown.

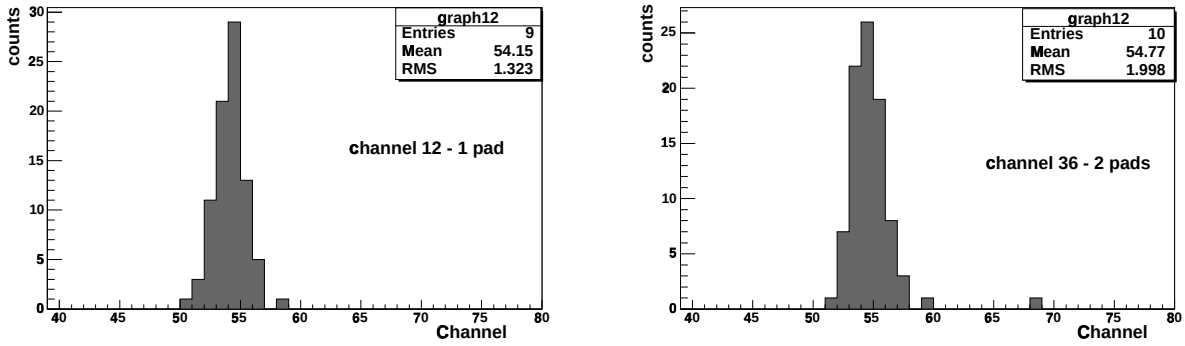

(a) (b)

FIG. 19: Spectrum from a $^{2}41$Am source obtained from channel 12, with only one pad connected (a), and from channel 36 with two pads connected (b).

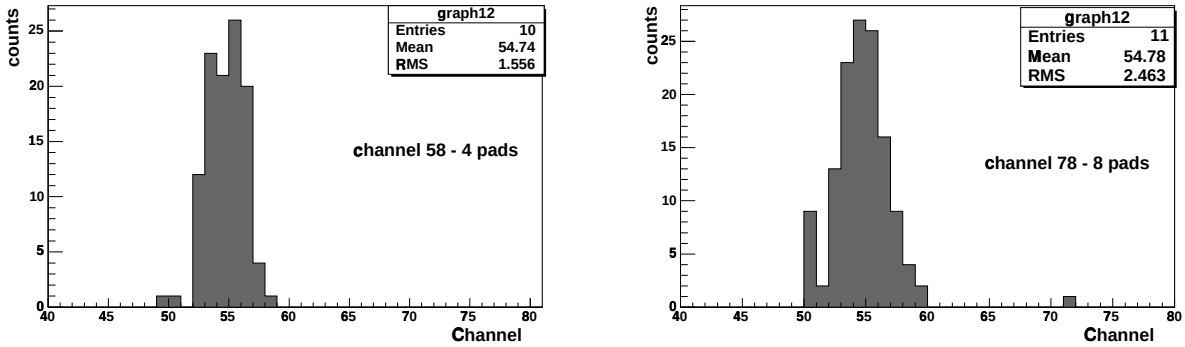

(a) (b)

FIG. 20: Spectrum from a $^{2}41$Am source obtained from channel 58, with 4 pads connected (a), and from channel 78 with 8 pads connected (b).

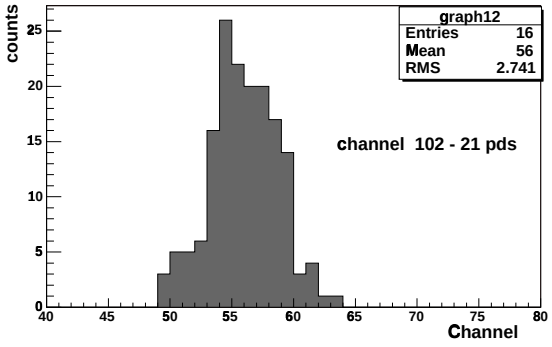

FIG. 21: Spectrum from a $^{2}41$Am source obtained from channel 102, with 21 pads connected.

From figures 19,20 and 21 it can be seen that the energy resolution deteriorates increasing the number of the readout pads, due to the increase of the sensor capacitance. If it assumed that the energy resolution is limited by the electronic noise, then the noise can be calculated knowing the RMS of the energy distribution:

$$Noise\ (RMS\ e-) = \frac{RMS(eV)}{3.6eV} \tag{14}$$

where 3.6 eV represent the energy required to create an electron-hole pair from and incident particle.